AN EXPERIMENTAL INVESTIGATION OF A TWO-DIMENSIONAL, SELF-SIMILAR, SUPERSONIC TURBULENT MIXING LAYER WITH ZERO PRESSURE GRADIENT

Hideo Ikawa, et al

California Institute of Technology

Prepared for:

Army Research Office-Durham

26 December 1973

ARO. 10863.1-E

AN EXPERIMENTAL INVESTIGATION OF A TWO-DIMENSIONAL, SELF-SIMILAR, SUPERSONIC TURBULENT MIXING LAYER WITH ZERO PRESSURE GRADIENT

FINAL REPORT

Hideo Ikawa and Toshi Kubota

July ~~October~~ 1, 1972 - September 30 1973

U. S. ARMY RESEARCH OFFICE -

DURHAM

Contract No. DAHC04-72-C-0038

CALIFORNIA INSTITUTE OF TECHNOLOGY

THE FINDINGS IN THIS REPORT ARE NOT TO BE CONSTRUED AS AN OFFICIAL DEPARTMENT OF THE ARMY POSITION, UNLESS SO DESIGNATED BY OTHER AUTHORIZED DOCUMENTS.

Unclassified

Security Classification

AD 774316

DOCUMENT CONTROL DATA - R & D

(Security classification of title, body of abstract and indexing annotation must be entered when the overall report is classified)

1. ORIGINATING ACTIVITY *(Corporate author)*

California Institute of Technology
Firestone Flight Sciences Laboratory
Pasadena, California 91109

2a. REPORT SECURITY CLASSIFICATION

Unclassified

2b. GROUP

NA

3. REPORT TITLE

An Experimental Investigation of a Two-Dimensional, Self-Similar, Supersonic Turbulent Mixing Layer with Zero Pressure Gradient

4. DESCRIPTIVE NOTES *(Type of report and inclusive dates)*

Final Report October 1, 1972 - September 31, 1973

5. AUTHOR(S) *(First name, middle initial, last name)*

Hideo Ikawa and Toshi Kubota

6. REPORT DATE	7a. TOTAL NO. OF PAGES	7b. NO OF REFS
December 26, 1973	24	16

8a. CONTRACT OR GRANT NO.	9a. ORIGINATOR'S REPORT NUMBER(S)
DAHC-72-C-0038	AROD-10863-1-E
b. PROJECT NO.	
c.	9b. OTHER REPORT NO(S) *(Any other numbers that may be assigned this report)*
d.	

10. DISTRIBUTION STATEMENT

Approved for public release; distribution unlimited.

11. SUPPLEMENTARY NOTES	12. SPONSORING MILITARY ACTIVITY
	U. S. Army Research Office-Durham Box CM, Duke Station Durham, North Carolina 27706

13. ABSTRACT

The effect of compressibility on the mixing layer was investigated at Mach number 2.47. Pitot pressure, static pressure and hot-wire surveys were made to investigate the mean flow and the fluctuation quantities. Similarities between supersonic and incompressible mixing layers are observed in normalized velocity profile, normalized power spectral density distribution and convection velocity distribution. Spreading rate, normalized shear stress and velocity fluctuation were found to be appreciably smaller than the respective incompressible results; e.g., the momentum thickness growth rates are 0.0073 and 0.035 for supersonic and incompressible flows, respectively. The difference between free and wall-bounded mixing layers is discussed. Development of turbulence structure of mixing layer with increasing Reynolds number was also investigated.

DD FORM 1 NOV 68 1473 REPLACES DD FORM 1473, 1 JAN 64, WHICH IS OBSOLETE FOR ARMY USE.

Unclassified

Security Classification

AD 774316

14. KEY WORDS	LINK A		LINK B		LINK C	
	ROLE	WT	ROLE	WT	ROLE	WT
Two-Dimensional Supersonic Turbulent Mixing Layer Zero Pressure Gradient Turbulence Structure of Mixing Layer Fluctuation Flow Field						

TABLE OF CONTENTS

List of Figures

List of Symbols

A	Area of porous plate (in^2)
b	Width of mixing layer (inch)
f	Frequency (Hz)
h	Step height behind upstream block (inch)
M	Mach number
$\dot{m}_{ACT}$	Actually injected mass flux through porous plate
p	Pressure (mm Hg)
p_o	Stagnation pressure (mm Hg)
p_{pl}	Plenum chamber pressure (mm Hg)
R	Correlation function
T	Temperature (^oR or ^oK)
U	Freestream velocity (ft/sec)
u, v, w	Velocity components
x, y, z	Axial, lateral, spanwise coordinate
$\bar{x}, \bar{y}, \bar{z}$	Incompressible coordinate
θ	Momentum thickness $= \int_{-\infty}^{\infty} \frac{\rho u}{\rho_e u_e} (1 - \frac{u}{u_e}) dy$ (inch)
θ_o	Initial momentum thickness of boundary layer at step corner (inch)
λ_e	Entrainment rate $= \rho_w v_w / \rho_e u_e$
σ	Spreading parameter ($\sigma y/x$)
ρ	Density of fluid ($slug/ft^3$)
τ	Shear stress or delay time of temporal correlation functions

Superscripts

$( )'$	Fluctuation quantity
$\overline{( )'^2}$	Mean squared fluctuation quantity
$(\tilde{\ })'^2$	Normalized mean squared quantity; $\tilde{g}'^2 = \frac{\overline{g'^2}}{\int \overline{g'^2}\, df}$

Subscripts

c Convection flow quantity

e Edge condition of TFML

L Local flow property

o Stagnation flow quantity

Definitions

F-T-F Boundary layer trip with fine grain sandpaper (carborandum C-320)

R-T-F Boundary layer trip with coarse grain sandpaper (Alum-Oxide C-320)

TFML Turbulent free mixing layer

TWML Turbulent wall (forced) mixing layer

Introduction

In the past two and a half decades, extensive investigations have been conducted on the theoretical and experimental problems of two-dimensional, self-similar, supersonic turbulent mixing layer. Many experimental investigations were made in the mixing region of jet and limited to the measurements of mean velocity profiles and growth rates of the turbulent mixing layer. These experiments were summarized by Maydew and Reed.[1] Two-dimensional mixing layers in wind tunnels were investigated by Roshko and Thomke[2] and by Sirieix and Solignac.[3] General conclusions of these investigations were that the spreading rate (and hence the mass entrainment rate) decreases with increasing Mach number and that the velocity profile can be reduced to the incompressible form when the lateral coordinate is scaled with the mixing-layer thickness (Mach number dependent).

On the other hand, the investigation of the two-dimensional, supersonic turbulent boundary layer with a massive injection of air by Fernandez[4] revealed that a different scaling law, namely, the Howarth-Dorodnitsyn integral transformation, was required to reduce the supersonic velocity profile to the incompressible form. When the integral scaling law was applied, the mass entrainment rate of the turbulent mixing layer was found invariant with Mach number, contrary to the findings of the former investigators. The two-dimensionality and the effect of the flow in the low-speed region of the former experiments were questioned by Fernandez in order to explain the observed differences.

The present investigation[5] of the two-dimensional, self-similar, supersonic turbulent mixing-layer structure, the investigation includes the measurement of the streamwise component of the fluctuation fields.

Description of Experiment

Wind Tunnel and Test Model

The experiments were conducted in the supersonic wind tunnel of the Graduate Aeronautical Laboratories, California Institute of Technology (GALCIT) with the nominal operational conditions of $M_e = 2.47$ (± 0.02), $p_o = 735$ mm Hg (± 5 mm Hg), $T_o = 27^oC$ ($\pm 3^oC$) and Reynolds number per inch of 2.3×10^5. The velocity and pressure fluctuations, measured in the undisturbed flow upstream of the step, were found to be 0.2% of freestream velocity and 0.1% of dynamic pressure, respectively. The wind tunnel is of the continuously-running type with closed circuit, which made the detailed survey of turbulent mixing layer possible.

The unique setup was employed in the present experiment in order to produce an ideal constant-pressure supersonic mixing layer with minimal interferences in the downstream of the rearward facing step. This condition was established by modifying the wind-tunnel test section as shown in Fig. 1. A stainless steel porous plate (0.25 x 2.00 x 8.00 with 10 micron grain size porosity) was installed at the bottom wall behind the step of the half nozzle block. A controlled amount of air was injected uniformly into the base region through the porous plate until pressure levels between the upstream and the base region become equalized, so that a flow free of shock or expansion at the step corner was created. Precise measurement of mass entrainment at the lower boundary of the mixing layer was also made possible with the present arrangement. The uniformity of injection through the porous plate was investigated under the pressure level of the actual test condition and the data obtained by a hot-wire probe are shown in Fig. 2 Spanwise survey showed jet-like flow directing toward both edges caused by pressure gradient which was subsequently eliminated by the fences installed on both sides of the porous plate.

Unfavorable pressure gradient induced by an abrupt termination of injection at the end of the plate (x = 8.00 inches) was eliminated by installation of the precisely contoured block simulating the streamline downstream of the injection plate. Boundary layer over the half nozzle block was tripped upstream of the throat to produce a fully developed turbulence. The surveys were made in a region of 1.0 inch upstream to 9.75 inches downstream of the step corner ($-100 \leq x/\theta_o \leq 975$). The relative positions of vertical and horizontal traverses were measured accurate to within 0.002 inch.

Mean Flow Measurements

Distributions of mean flow properties were measured by the conventional Pitot and static pressure probes. In order to monitor the uniformity of the flow field during the test, one of the side fences was instrumented with rows of 40 static pressure taps. Velocity, Mach number, density profiles and integral quantities were computed by the Pitot-Rayleigh formula with constant total temperature assumption across the mixing layer. Total temperature deviation of ± 2% of the mean value was measured with hot-wire operating as a resistance thermometer. The net total energy flux was integrated to be zero across the shear layer.

Fluctuation Flow Field Measurements

Turbulent fluctuations of the streamwise component were measured by the Shapiro-Edward constant-current hot-wire anemometer. Hot-wire probes were made of 0.00005 inch diameter platinum - 10% wire with length to diameter ratio of 120 to 200. In order to account for the attenuation of amplifier response at high frequency and the thermal lag response of wire to the fluctuation flow field, power spectral density distributions of turbulent fields were measured by the Tektronix Spectrum Analyzer Type 1L5, and the turbulent intensities were then determined by integrating

the spectral distributions with application of appropriate corrections. The magnitudes of mass flux and total temperature fluctuations were computed by the Morkovin's curve fitting technique described by Gran.[6] Velocity and static-temperature fluctuation intensities within the mixing layer were ca;ci;ated bu Kistler's method,[7] derived for the supersonic turbulence, extended into the subsonic regime with an assumption that pressure fluctuations have negligible contribution compared with vorticity and entropy fluctuations.

Crosscorrelation measurements of two hot-wire signals, arranged tandemly along the rays of constant velocity, were made to determine the convection velocity profiles. The measurements were taken in real time as the signals were processed with the SAICOR Correlation and Probability Analyzer (Model SAI 43A) during the experiment. Detailed descriptions of test and data reduction procedures are given in Ref. 5.

Results and Discussion

Preliminary Mean Flow Measurements

Preliminary investigations of the supersonic turbulent free mixing layer behind a rearward-facint step were conducted to delineate the nature of the flow field. The porous bottom wall through which air is injected was positioned at two heights of 1.0 and 0.5 inch below the surface of the upstream block. The streamline block was not used.

With h = 1.0 inch, the injection rate of 0.01 was required to bring the mixing layer straight out. The static pressure distribution was constant from the corner to the station x = 5.0 and it was followed by a decrease in pressure, resulting in about 20% pressure drop at the end of the injection plate. The flow was found self-similar in the region of constant pressure. The growth rate of momentum thickness ($d\theta/dx$)

computed from the velocity profile was 0.007, less than the actual injection rate.

With the porous wall positioned at h = 0.5 inch, the actual injection of λ_e = 0.0068 was required to establish the self-similar flow in the same region. The pressure was constant up to x = 4.0 and the positive pressure gradient was noted beyond this station. The velocity distribution and $d\theta/dx$ were identical with the h = 1.0 inch case in the constant pressure region indicating that the scale of turbulent free mixing layer is independent of the step heights. The influence of the step height was found to be introduced by the flow interaction between the lower edge of the mixing layer and the bottom wall. The observations suggested that the ideal condition may be established by tailoring the wall shape beyond the termination of injection, which led to the design of the streamline block. The important finding of the preliminary test was that the entrainment of the supersonic TFML in the nearly constant pressure region was much lower than the incompressible TFML of Liepmann and Laufer.[8]

Mean Flow Data

The self similarity of two-dimensional turbulent mixing layer with zero pressure gradient must satisfy two criteria; the spreading of the mixing layer grows linearly with streamwise distance (x) and the mass entrainment rate through the lower boundary of the mixing layer equals the growth rate of momentum thickness ($\lambda_e = d\theta/dx$).

The self-similar flow of the present investigation was established approximately 275 θ_o downstream of the step. The comparison of the normalized velocity profiles taken over the range of 375 θ_o to 975 θ_o is shown in Fig. 3. The velocity profiles, normalized with the momentum thickness and matched at the dividing streamline, collapsed to a single

curve. The profile taken at $x/\theta_o = 975$, measured over the streamline block, was normalized with the effective TFML momentum thickness computed at this station. Under this normalization, the profile matched with the other TFML profiles, except near the wall where the redevelopment of boundary layer was displayed. The conclusive evidence of the self-similarity is observed in the map of velocity field shown in Fig. 4. The linear growth of mixing layer is evident beyond x = 2.75 inches and the virtual origin is determined at the convergence point of the constant-velocity lines. Initial turbulent boundary layer with thickness of about 0.135 inch was formed at just upstream of the step corner. The corresponding initial momentum thickness was approximately 0.01 inch and the presence of finite boundary layer delayed the development of self similar TFML. The significance of supersonic TFML is that the spreading rate was found to be smaller than that for the incompressible flow case. The spreading rate (dy/dx) computed between the velocity ratio (u/u_e) of 0.1 to 0.9 were approximately 0.064 for $M_e \cong 2.47$ flow and 0.16 for the incompressible flow.[8] The conventional spreading parameter, σ, was found to lie between 27 and 29.

The correlation of the momentum thickness growth rate and the mass entrainment rate was established experimentally, thereby verifying that the mixing layer of this investigation was two-dimensional and self-similar. The mass entrainment rate was determined by dividing the measured total injected mass by the injection plate area and the free-stream mass flux, i.e., $\lambda_e = \dot{m}_{ACT}/A_k u_e = \rho_w v_w/\rho_e u_e$. The measured mass entrainment rate was found approximately 0.0073. The comparison between the measured λ_e and the development of momentum thickness is shown in Fig. 5. The momentum thickness shows the linear growth beyond X = 2.75 inches, and the slope of the momentum thickness

distribution is $0.0071 \leq d\theta/dx \leq 0.0075$ within the experimental accuracy. The equality of two slopes, θ-distribution and mass entrainment distribution, established the relation, $\lambda_e = d\theta/dx$. Note that the growth rate of momentum thickness of $M_e = 2.47$ flow is also appreciably smaller and it was found to be approximately one-fifth of the incompressible value ($d\theta/dx = 0.0073$ versus $d\theta/dx = 0.035$).

In order to compare the velocity profiles of supersonic and incompressible TFML, the velocity profile was normalized by using the two previously suggested scaling laws. The velocity profile comparison is shown in Fig. 6. The integral transformation suggested by Fernandez[4] is not satisfactory to the flow of the present investigation; there is too much contraction in the subsonic region but very little scaling effect is noted in the supersonic region. On the other hand, an excellent matching of two profiles was observed by the linear scaling. This finding suggests that a universal velocity for the turbulent free mixing layer flow may exist. Of course, this observation must be substantiated by further experiments in the higher Mach number, preferably $M_e \geq 5.0$.

Scaling of supersonic TFML was examined by many investigators[2] in order to correlate the scaling parameter with physically measurable properties such as density ratio, Mach number, etc. They have shown that the spreading parameter can be represented by the density ratio across the layer, although the exact nature of the relation has not been firmly established. Brown and Roshko[9] found in the experiment of hetergeneous gas (binary-incompressible) mixing that the spreading parameter did not vary with the density ratio as much as supersonic flow did with the same density ratio. Therefore, they concluded that the observed variation in supersonic flow must have come from the compressibility effect. It was

noticed that most of the density variation occurs in the supersonic region of the TFML, flow field above the dividing streamline, and remains relatively constant in the subsonic region. Considering the foregoing density distribution and assuming a universal velocity profile, the momentum balance across the dividing streamline will yield the relation that the variation in spreading rate of the adiabatic supersonic TFML can be reasonably approximated with the density ratio relation established by Alber.[10] Alber showed that the mixing layer spreading rate is proportional to the density ratio and the momentum thickness growth rate is proportional to the square of the density ratio.

Shear stress distributions plotted against the velocity ratio in the self similar TFML, computed from the mean flow data using the method described by Fernandez,[4] were found to be identical to the other mixing layer type of flow (for example, see Ref. 4) so that the figure is not presented. The peak value of the turbulent shear stress occurred slightly above the dividing streamline near $u/u_e \cong 0.62$. For the truly asymptotic TFML, the locations of maximum shear stress and dividing streamline should coincide. The discrepancy is attributable to the presence of finite initial boundary layer. The peak shear stress, normalized by twice the freestream dynamic pressure and entrainment rate ($\tau_{max}/\lambda_e \rho_e u_e^2$), was approximately 0.385 and was constant with streamwise station. This value is slightly higher than the incompressible value of Liepmann and Laufer[8] ($\cong 0.34$). However, since $\lambda_e(M)$ decreases with an increasing Mach number, the normalized shear stress, $\tau_{max}/\rho_e u_e^2$, decreases with increasing Mach number. For example, $\tau_{max}/\rho_e u_e^2$ of the present investigation was approximately 0.0028 whereas the incompressible value[8] was approximately 0.012.

Comparison of significant properties between the incompressible and the supersonic mixing layers of the present investigation is listed in Table 1.

Comparison of Supersonic TFML and TWML

Uniform injection of mass into turbulent boundary layer (TBL) creates a flow pattern which develops from the boundary layer to the mixing layer type. Supersonic experiments of this type was undertaken by Fernandez,[4] who found that a flow field similar to the mixing layer can be created when the uniform injection rate approached $\lambda_e = 0.035$, the value comparable to the incompressible TFML with zero pressure gradient. Scaling the velocity profiles with Howarth-Dorodnitsyn transformation ($\bar{y} = \int \frac{\rho}{\rho_e} dy$), Fernandez has demonstrated that the velocity profiles of supersonic flow with various blowing rates can be reduced to match with the subsonic velocity profiles of respective blowing rates. Fernandez terminated the experiments when the blowing rate reached the value of 0.029. For this blowing rate, the transformed velocity profile matched well with the incompressible TFML of Liepmann and Laufer.[8] It was then concluded that the upper limit of the entrainment rate of supersonic turbulent mixing layer is equal to the incompressible value, $\lambda_e = 0.035$. Then it follows that the growth rate of momentum thickness in the similar turbulent mixing layer is independent of Mach number (θ is invariant under Howarth-Dorodnitsyn Transformation).

The present investigation, conducted in the same wind tunnel used by Fernandez, produced the results contrary to the case observed by Fernandez. It must be noted that the primary difference between the mixing layer flows investigated by Fernandez and the present author was that the flow field of the former investigation was always bounded by the wall, whereas the latter was completely unbounded. Therefore, the mixing

layer flow created by massive injection into the TBL is classified in the present text as the turbulent wall mixing layer (TWML) in order to distinguish it from the turbulent free mixing layer (TFML) flow of the present investigation.

The mass entrainment characteristics of TWML can be investigated by reanalyzing the velocity profiles of various injection rates in the physical coordinate system. The common reference point was selected at $u/u_e = 0.6$, near the dividing streamline, instead of the wall. Fernandez' data replotted in this manner revealed that the velocity profile could be divided into two distinct region, i.e., above and below the dividing streamline as shown in Fig. 7. The dividing streamline was defined near the sonic point by mass balance. The velocity profile in the supersonic layer above the dividing streamline appeared to have developed into the shape, which is identical to the TFML, with blowing rate as low as 0.01. The external profiles remained nearly unchanged with further increase in the blowing rate. The forced mass entrainment was confined to the subsonic region between the dividing streamline and the wall. The thickening in the subsonic region was found to be directly proportional to the injection rate and appeared to be an exact inverse of the contraction of the y-coordinate by the Howarth-Dorodnitsyn transformation. Therefore, the TWML is found capable of entraining more mass than the fully developed TFML.

The forced mixing layer experiment in supersonic flow using the 20° backward sloping ramp was performed by Collins.[11] In order to achieve a straight mixing layer with zero pressure gradient, the injection rate of 0.0176 was needed for a model with the streamline block. Once again, the velocity profile in the supersonic layer matched with the one

of the TFML but the subsonic region below the dividing streamline was appreciably altered. In fact, the integration of mass flux confirmed that the difference in mass entrainments between TWML and TFML can be accounted for in the tail profile. So far no turbulent mixing layer with forced entrainment large enough to alter the flow pattern in the supersonic side of velocity profile has been observed. It is uncertain at this time if the dividing streamline will always remain on or below the sonic point and if the supersonic layer profile of TWML will ever be altered appreciably.

Turbulent Field Data

The present investigation revealed that at least the following three conditions must be satisfied before the supersonic turbulent mixing layer can be classified as the fully developed asymptotic form: 1) constancy of spreading rate with streamwise distance; 2) turbulent spectra of broad-band character with no peak signal; and 3) constancy of total turbulence energy level. Requirement of the second criteria will be discussed later.

The self-similarity of the turbulence field was established by the turbulent spectral surveys made at several stations along the constant velocity ray. The frequency and the spectral intensity were normalized by the mean flow quantity, u_I/θ. Velocity fluctuation spectra measured nearly along the dividing streamline are shown in Fig. 8. The normalized spectral distributions falling onto a single curve assured the self-similarity of the turbulent field. Since the measurements were taken along the constant velocity raty and the momentum thickness was found to grow linearly, the spectral normalization with the local momentum thickness also implied that the integral scale of turbulence was also a linear function of streamwise

distance. Spectral distribution was observed to be a broad-band type with no discernible peak. Streamwise constancy of turbulent intensity was also established after it was corrected for the instrumentation response. Thus, the turbulence field was found to be fully developed and self similar beyond the longitudinal station, $x/\theta_o \geq 375$.

Velocity fluctuation spectra taken laterally across the core of the mixing layer reduced to a single curve when they were normalized with the local velocities as shown in Fig. 9. This implied that the characteristic frequency across the mixing layer is inversely proportional to the local mean velocity, u_L. The spectra was flat up to $f\theta/u_L \cong 2 \times 10^{-2}$ and accompanied with the initial decay inversely proportional to frequency. The final decay at higher frequencies appears to follow $f^{-5/3}$. In order to compare the present results with the incompressible turbulent spectra, the frequency and intensity coordinates were renormalized with the width of mixing layer determined by the slope-intercept method as suggested by Batt et al.[12] The new scale is shown below the original one. The incompressible spectra of Batt et al. fall onto the present data. Excellent agreement of the low frequency range of spectra is observed and the energy carrying component matched near the Strouhal number ($2\pi fb/u_L$) of unity. The high frequency components of incompressible data fall off with -2 power, but it was also reported by other investigators that the incompressible spectra also decay with -5/3 power. Considering the difficulty encountered in the hot-wire survey in the supersonic turbulence, the turbulence spectra of supersonic and incompressible TFML may be considered qualitatively identical.

The RMS intensities of streamwise velocity and static temperature fluctuation distributions, normalized with the respective local flow properties, are shown in Fig. 10. Scattering of data is inevitable in this type of

experiment, thus the confidence level of the computed data is somewhat reduced when compared with the mean flow measurements. However, ensemble of many data points established a certain trend of physical measurements associated with the flow field of realizable turbulence. The maximum RMS intensity of streamwise velocitu fluctuation ($\sqrt{\overline{u'^2}}/u_L$) was found to be approximately 8 to 9% of local mean velocity and occurred near the maximum gradient of velocity profile. The absolute maximum RMS fluctuation of approximately 5 to 6% of freestream velocity ($\sqrt{\overline{u'^2}}/u_e$) was observed near $y/\theta = 1.5$ and shown as the shaded band of curve. The corresponding peak values in incompressible flow reported by various investigators lie between 16 to 20% of u_e. Based on these values, the maximum intensity of RMS velocity fluctuation of supersonic TFML is approximately one-third of the subsonic TFML. This finding may offer a partial explanation for the observed reduction in the supersonic TFML growth rate. It is expected that the general relationship between the remaining velocity fluctuation components (RMS of v' and w') in the supersonic TFML should not be greatly different from that observed in the subsonic TFML. Thus it is speculated that the relative kinetic energy of velocity fluctuation at $M = 2.5$ is also expected to be lower than the incompressible value.

The static temperature fluctuation profile normalized with the local mean static temperature peaked in the supersonic side of the layer near the point of the maximum gradient of mean static temperature ($y/\theta \cong 3$). The peak RMS temperature fluctuation is approximately 8.5% of T_L as shown in Fig. 10b. The plateau near $y/\theta \cong -2$ is speculated to be produced by the difference in the turbulent transport mechanisms between the momentum fluctuation and the thermal fluctuation. Although

the exact nature of observed phenomenon was unknown, it appeared repeatedly to indicate that this was a physically observable phenomenon. Under the assumption of negligible pressure fluctuation compared with the vorticity and entropy fluctuations within the highly turbulent shear layer, the temperature fluctuation is precisely a negative of the density fluctuation ($T'/T_L = -\rho'/\rho_L$), but RMS fluctuation of density and temperature are the same ($\sqrt{\overline{T'^2}}/T_L = \sqrt{\overline{\rho'^2}}/\rho_L$).

The streamwise velocity and static temperature fluctuation were found highly anti-correlated at the freestream edge of the TFML ($R_{\overline{u'T'}} \leq -0.7$). The correlation function approached to zero (uncorrelated) as the dividing streamline was approached from the high speed mixing layer edge and became positive in the subsonic layer. Relatively high correlation ($R_{\overline{u'T'}} \geq 0.7$) was observed near $y/\theta \cong -2$.

The combined intensity of all fluctuating modes of supersonic TFML were found large but an appreciable amount of energy appeared to have dissipated into thermal energy as observed in the high temperature fluctuation profile. Therefore, it is speculated that the vorticity mode of fluctuation which mainly contributes to the growing of the turbulent field is left with relatively low kinetic energy. The observed phenomena may supply a clue to the decreasing trend of the spreading rate associated with the supersonic TFML.

Convection velocity of the turbulent field was determined by the measurement of space-time correlation of two hot-wire signals along the ray of constant u/u_e. The definition of convection velocity adopted by Wills[13] was given as $u_c = \partial x/\partial \tau$ at the point where $(\partial R/\partial x)_{\tau = \text{const}} = 0$. This point can be determined by finding the tangency point of crosscorrelation functions with their envelope in the R-τ plot. The convection

velocities of broad band turbulence across the TFML were compared with the mean velocity and shown in Fig. 11a. The turbulence convection velocity above the dividing streamline was found to be smaller than the mean velocity and below the dividing streamline larger than the mean velocity. Both the turbulent convection and the mean velocities were identical near the dividing streamline, where the turbulence production term was maximum. The subsonic data obtained by Wills[13] and Bradshaw[14] in the axisymmetric jet mixing layer showed the identical relation with the mean velocity as the present results. Subsonic 2-D mixing layer results obtained by Wygnanski and Fiedler[15] showed the consistently lower convection velocity throughout the TFML.

The convection velocities of selected frequency components of turbulence at $u/u_e \cong 0.90$ (maximum unresolved turbulence signal), $u/u_e \cong 0.61$ (near the dividing streamline) and $u/u_e \cong 0.25$ were measured by application of two Hewlett-Packard Wave Analyzers as narrow-bandpass filters before the two signals were correlated and the results are shown in Fig. 11b. At point A ($u/u_e \cong 0.90$), the convection velocity was lower for low frequency components and monotonically increases with frequency. The mean convection velocity at this lateral position was approximately $0.80\ u_e$, and the energy carrying turbulent components were concentrated near the frequency domain of 25K to 100 KHz. The unresolved power spectral distribution in this frequency domain appeared to decay proportional to f^{-1}. At point B ($u/u_e \cong 0.61$), all frequency components of turbulence were convecting with the same speed. Convection velocities of the turbulence components below the dividing streamline decreased with frequency. Note that large scale turbulence of TFML appeared to

be convecting with relatively constant speed of the dividing streamline across the layer. Jones, et al.[16] also observed qualitatively the same results in the incompressible two stream mixing layer. This observation suggests that the small scale turbulence adjusts to the local environment faster than the large scale eddies as the turbulence field convects downstream.

The present and Wills' results indicate that the switching point of the relative velocity occurred very close to the dividing streamline of TFML. In fact, the results suggest that the large-scale turbulence is created in the vicinity of the dividing streamline by the maximum shear stress and maximum velocity gradient. The production rate, $\tau \frac{\partial u}{\partial y}$, determined from the mean flow values peaks at $u/u_e \cong 0.55 \sim 0.60$.

Two Dimensionality of TFML

The self-similar, two-dimensional TFML criteria were satisfied in the section of the mean flow. In addition, two-dimensionality of turbulent field was also assured by the measurements of crosscorrelations in the spanwise displacements of two hot-wire probes. The measurements were taken near the point in the mixing layer where the maximum unresolved turbulent signal was detected. Unresolved space-time correlations are shown in Fig. 12. The delay-time at the peak correlation function did not shift with Δz. The distributions of correlation of the spanwise separation were enveloped within the skirt of autocorrelation function and very little distortion of the flow pattern was observed. These two facts confirmed that the turbulent flow field of this investigation was perfectly two dimensional.

Development of Turbulence Structure of TFML

When hot-wire surveys were conducted with an operating condition of $p_o = 610$ mm Hg, a peaking of signal near frequency of 5 KHz appeared

in the turbulence spectra taken in the TFML. The cause of this peculiarity was traced to the upstream conditions, laminar-turbulent transitional boundary layer instability or some Reynolds number dependent disturbance in the boundary layer, which influenced the downstream flow. In order to observe the development of turbulence structure, the response of turbulent spectra to the total pressure variation was investigated in the TFML. Since all other operating conditions remained unchanged, the total pressure variation implied the direct Reynolds number variation. The unresolved turbulent energy spectra were normalized with the integrated quantity.

The boundary layer was tripped with a strip of fine grain sandpaper. The spectra taken with p_o = 500 mm Hg are shown in Fig. 13a. The spectra were accompanied by pronounced peaking near f = 5 KHz (peak shift is due to X_E-normalization), which signifies the passage of high energy carrying organized eddies in the preferred frequency range. No significant development of medium to small scale turbulence was noted (oddly, it followed the $f^{-5/3}$ law immediately following the peak). The presence of large scale periodic motion was also detected by autocorrelation measurements. The intensity of integrated spectra decreased with the axial distance.

The spectra taken with p_o = 610 mm Hg are shown in Fig. 13b. Peaking of spectra near 6 KHz persisted but considerable development of higher frequency energy carrying component was also observed. This observation implies that this flow condition is the followup stage of the previous flow field. The agreement of the data beyond x = 4.75 is excellent, indicating that the high frequency components develop as in a self-similar flow. The passage of large scale wave-like motion, which

was less pronounced in intensity compared to the previous condition, was also detected by autocorrelation measurements. The integrated intensities were found relatively constant with X.

When the total pressure was increased to p_o = 900 mm Hg, the previously observed peak vanished completely and the broad band spectra of turbulence was obtained as shown in Fig. 13c. The high frequency components of this spectra distribution was found identical to the spectra taken with p_o = 610 mm Hg. No organized wave-like motion was detected by the autocorrelation measurement.

The operation of the tunnel was restored to the total pressure of one atmosphere (p_o = 735 mm Hg) and the boundary layer trip was replaced with a strip of coarse grain sandpaper. With these combined operating conditions, the signal peaking was eliminated and the entire spectra were found to be identical with the data taken with p_o = 900 mm Hg. Self-similarity of the turbulence field was evident in these measurements.

Disappearance of spectral peaks with the increase in Reynolds number and the roughness of the boundary layer trip indicates that the structure of fully developed supersonic TFML consists of a randomly fluctuating field with no large scale wave motion in a preferred frequency range. On the other hand, Brown and Roshko[9] visually observed the existence of quasi-periodic large scale motion in the incompressible TFML, which indicates a marked difference between subsonic and supersonic turbulent mixing layers.

Conclusions

The present investigation revealed that the turbulent free mixing layer was found to be strongly dependent upon the compressibility of the supersonic flow. The supersonic TFML was found to possess the

characteristics similar to the incompressible TFML but their magnitudes were considerably lower than the incompressible values. Similarities of the turbulent properties between the supersonic and the incompressible flows were: (1) the mean velocity profile that suggests the existence of a universal velocity profile, (2) the convection velocity distribution and its frequency dependence, (3) the normalized spectral density distribution of the streamwise velocity fluctuation, (4) the linear growth of the mixing layer with axial distance and (5) the equality of entrainment rate and growth rate of momentum thickness. Within the experimental accuracy, $\tau_{max}/\lambda_e \rho_e u_e^2$ may be considered constant with the value which lies between 0.34 and 0.385. Decreasing trends of the magnitudes with increasing supersonic Mach number were observed (1) in the spreading rate and the growth rate of momentum thickness, (2) in the RMS intensity of velocity fluctuations and (3) in the normalized shear stress, $\tau_{max}/\rho_e u_e^2$.

Observations suggest that the turbulence is created near the dividing streamline where the production term is maximum. Small scale turbulence adjusts quickly to the new local environments but the large scale eddies throughout the layer convect with the velocity of the dividing streamline.

It was found that the wall bounded mixing layer, created by the massive injection into the turbulent boundary layer, can entrain more mass than the free mixing layer created by the natural process. The thickening of the TWML below the dividing streamline is proportional to the injection rate.

Table I

Comparison Between Incompressible and Supersonic Two-Dimensional Turbulent Free Mixing Layer Properties

	Incompressible[8]	Supersonic (M = 2.47)
dy/dx $(.10 \leq u/u_e \leq .90)$	0.016	0.064
$d\theta/dx = \lambda_e$	0.035	0.0073
σ	12	$27 \sim 29$
$\tau_{max}/\lambda_e \rho_e u_e^2$	0.34	0.385
$\tau_{max}/\rho_e u_e^2$	0.012	0.0028
ρ_w/ρ_e	1.0	0.45
$\sqrt{\overline{u'^2}}/u_e\|_{max}$	$0.16 \sim 0.18$	$0.05 \sim 0.06$

References

1. Maydew, R. C. and Reed, J. F., "Turbulent Mixing of Axisymmetric Compressible Jet (in the Half-Jet Region) with Quiescent Air," Sandia Corp., SC-4764 (RR), March 1963.

2. Roshko, A. and Thomke, G. L., "Results of Pilot Experiment on Supersonic Free Shear Layers, "McDonnell Douglas Astronautics Company Report, DAL, Oct. 8, 1968.

3. Sirieix, P. M. and Solignac, J. L., "Contribution a L'Etude Experimental De La Couch De Melange Turbulent Isobare D'un Ecoulement Supersonique," Office National D'Etudes Et De Recherches Aerospatiales, T. P. No. 327, 1966.

4. Fernandez, F. L., "Two-Dimensional Viscous Flows with Large Distributed Surface Injection," Parts I, II, and III. Ph.D. Thesis, California Institute of Technology, 1969.

5. Ikawa, H., "Turbulent Mixing Layer Experiment in Supersonic Flow," Ph.D. Thesis, California Institute of Technology, 1973.

6. Gran, R. L., "Step Induced Separation of a Turbulent Boundary Layer," Ph.D. Thesis, California Institute of Technology, 1970.

7. Kistler, A. L., "Fluctuation Measurements in a Supersonic Turbulent Boundary Layer," Physics of Fluids, Vol. 2, No. 3, pp. 290-296, May-June 1959.

8. Liepmann, H. W. and Laufer, J., "Investigations of Free Turbulent Mixing," NACA TN 1257, 1947.

9. Brown, G. A. and Roshko, A., "The Effect of Density Difference on the Turbulent Mixing Layer," AGARD-CP-93, AGARD Conference Proceedings No. 93 on Turbulent Shear Flows, pp. 1-23, 13-15 September 1971.

10. Alber, I. E., "Integral Theory for Turbulent Base Flows at Subsonic and Supersonic Speed," Ph. D. Thesis, California Institute of Technology, 1967.

11. Collins, D. J., Unpublished data.

12. Batt, R. G., Kubota, T., and Laufer, J., "Experimental Investigation of the Effect of Shear-Flow Turbulence on a Chemical Reaction," AIAA Reacting Turbulent Flow Conference, June 17, 1970.

13. Wills, J. A. B., "On Convection Velocities in Turbulent Shear Flow," JFM Vol. 20, part 3, pp. 417-432, 1964.

14. Bradshaw, P., Ferriss, D. H., and Johnson, R. F., "Turbulence in the Noise-Producing Region of a Circular Jet," JFM, Vol. 19, Part 4, pp. 591-624, 1964.

15. Wygnanski, I. and Fiedler, H. E., "The Two-Dimensional Mixing Region," JFM Vol. 41, p. 329, 1970.

16. Jones, B. G., Planchon, H. P. and Hammersley, R. J., "Turbulent Correlation Measurements in a Two Stream Mixing Layer," AIAA Journal, Vol. 11, No. 8, pp. 1146-1150, August 1973.

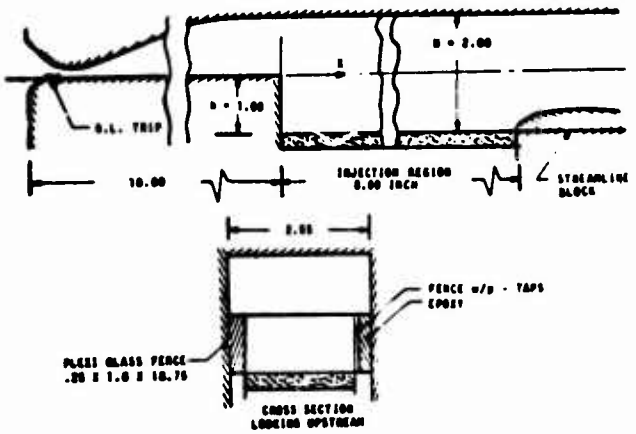

Figure 1. Test Section Configuration

M_e @ 2.47 P_0 = 735 mmHg T_0 = 540°R $R_e/_L$ = 2.3×10^5/in

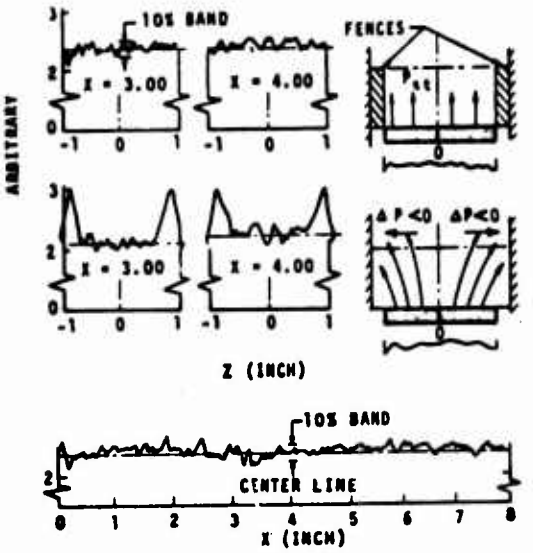

Figure 2. Flow Uniformity Through Porous Plate

Hot-Wire Survey 0.5" Above Surface

10μ Grain Stainless Steel Porous Plate

.25" x 2.00" x 8.0" P_{PL} = 320 mmHg P_s = 46 mmHg

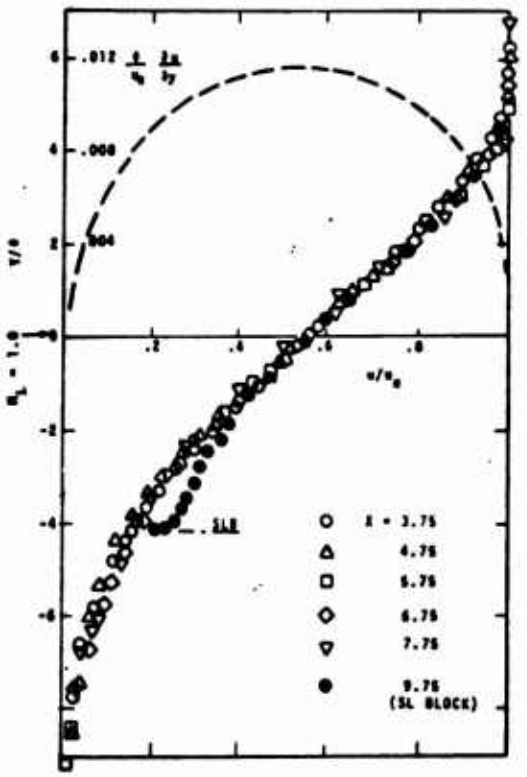

Figure 3. TFML Velocity and Velocity Gradient Profiles

M_e = 2.47 λ_e = 0.0073 P_0 = 735 mmHg R-T-F

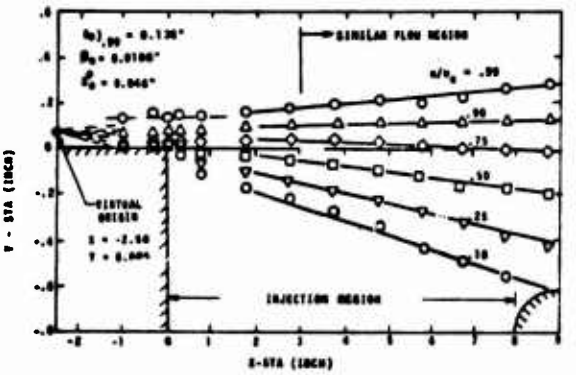

Figure 4 TFML Longitudinal Velocity Distributions

M_e = 2.47 λ_e = 0.0073 P_0 = 735 mmHg R-T-F

dy/dx = 0.064 for M_e = 2.47 } $.10 \leq u/u_e \leq .90$

dy/dx = 0.16 for M=0 (Ref. 8) }

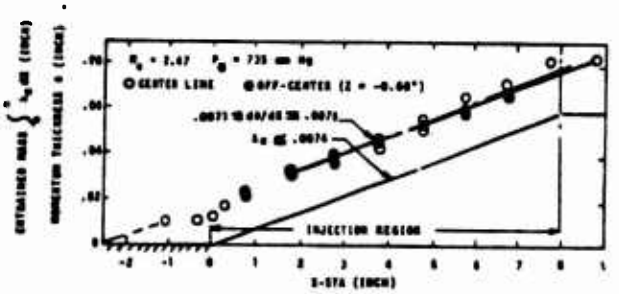

Figure 5. TFML-Comparison of Momentum Thickness Distribution vs. Entrained Mass Distribution

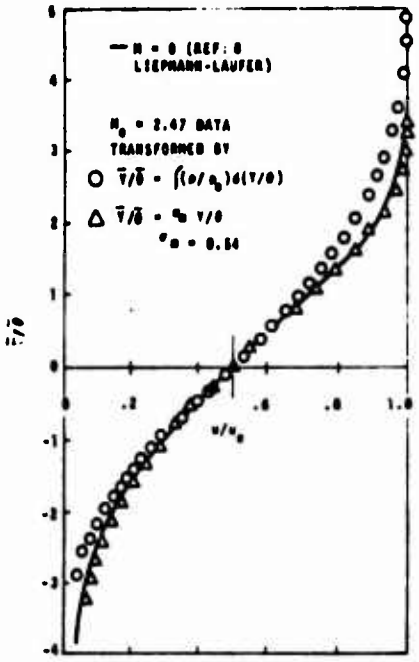

Figure 6. Linear and Integral Scaling of Supersonic Velocity Profile

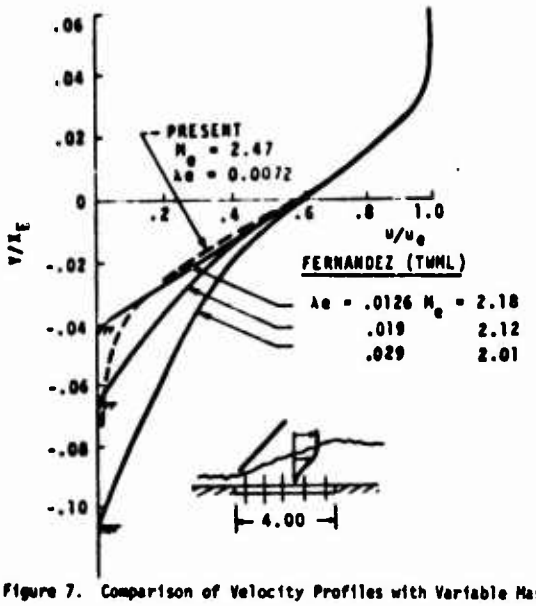

Figure 7. Comparison of Velocity Profiles with Variable Mass Injection Rates Through Flat Plate Model.

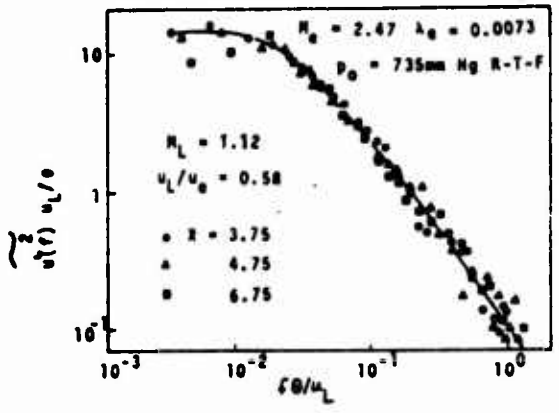

Figure 8. Similar Flow Spectra-Streamwise Velocity Fluctuation.

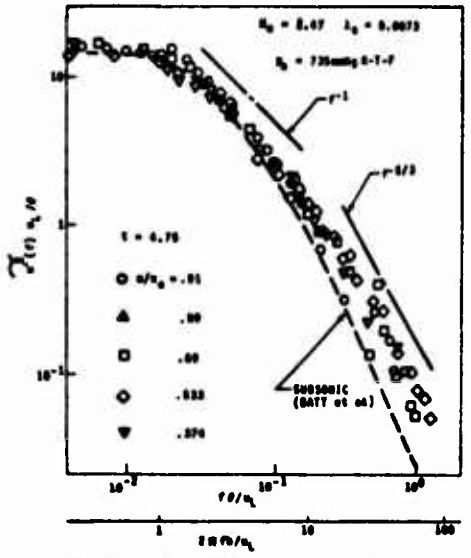

Figure 9. Comparison of Supersonic and Incompressible Streamwise Velocity Fluctuation Spectra

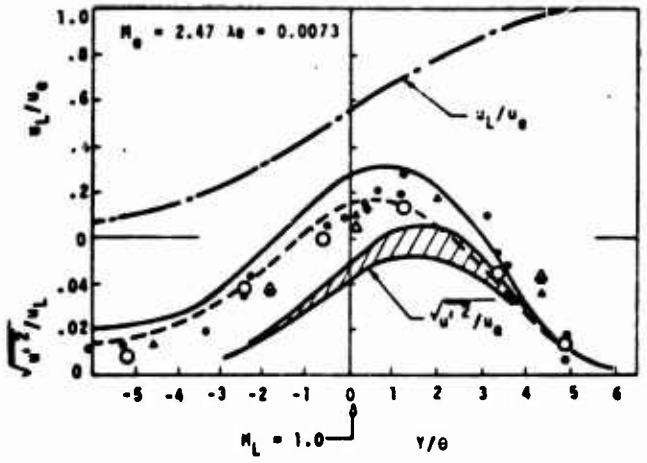

Figure 10a. Streamwise Velocity Fluctuation Profile.

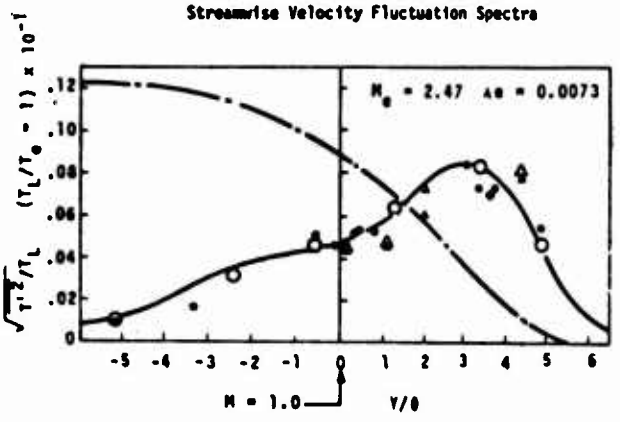

Figure 10b. Static Temperature Fluctuation

Etc. Measurements - M_A = 50usec -- M_A Variable

Spectra Measurements ○ X = 4.75 ◇ X = 6.75 P_o = 735 mmHg △ X = 4.75 P_o = 610 mmHg

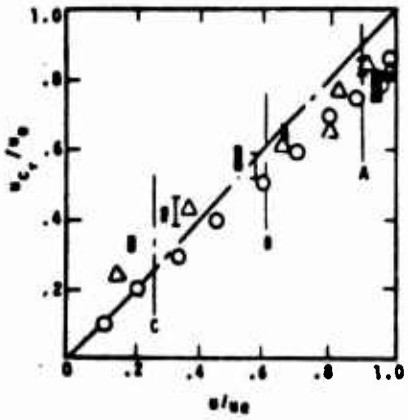

Figure 11a. TFML Streamwise Turbulent Convection Velocity vs. Mean Velocity

M_e = 2.47: ▩ P_o = 610 mmHg I P_o = 735 mmHg

△ Willis u_{Jet} = 330 ft/sec (ML in Axi-Sym Jet)

○ Wygnanski Fiedler M = 0 (2-D ML)

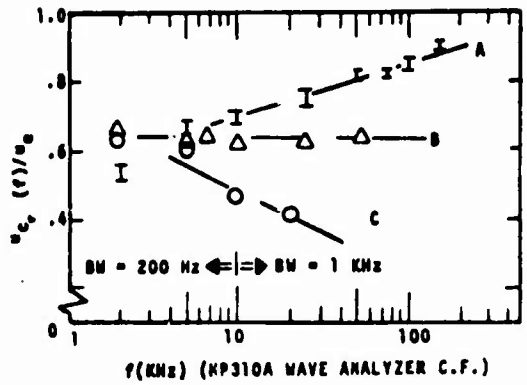

Figure 11b. Convection Velocity of Selected Frequency Components

I u/u_e = .9 △.6 ○.25

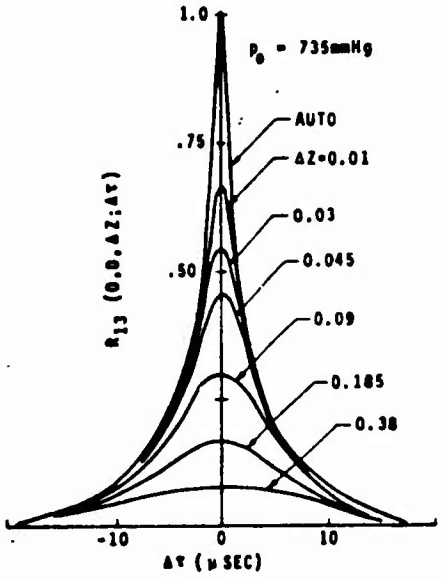

Figure 12. Spanwise Space Time Correlation Functions of Streamwise Flow Component.

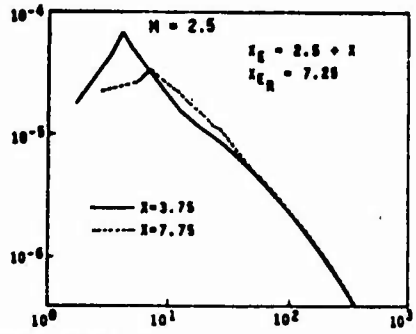

a. P_o = 500 mmHg F-T-F

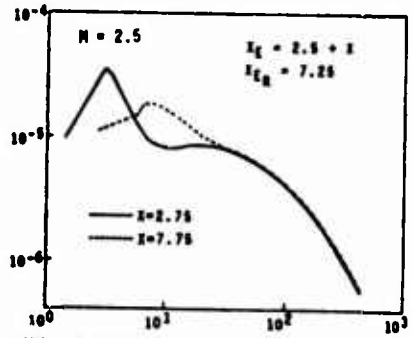

b. P_o = 610 mmHg F-T-F

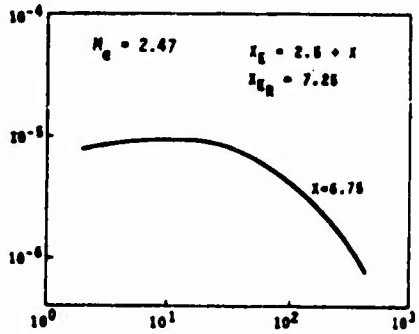

c. P_o = 900 mmHg F-T-F and P_o = 735 mmHg R-T-F

Figure 13. Energy Spectra With Variable Total Pressures